Available online at www.sciencedirect.com
ScienceDirect
Metabolism Clinical and Experimental 59 (2010) 554–560
Metabolism
Clinical and Experimental
www.metabolismjournal.com

Analysis of transcriptome and metabolome profiles alterations in fatty liver induced by high-fat diet in rat

Zuoquan Xie[a,c,1], Houkai Li[b,1], Ke Wang[c,d], Jingchao Lin[b], Qi Wang[c], Guoping Zhao[c], Wei Jia[b,e,*], Qinghua Zhang[a,c,*]

[a]State Key laboratory of Medical Genomics and Shanghai Institute of Hematology, Ruijin Hospital, Shanghai Jiao Tong University School of Medicine, Shanghai 200025, PRC
[b]School of Pharmacy, Shanghai Center for Systems Biomedicine, Shanghai Jiao Tong University, Shanghai 200240, PRC
[c]National Engineering Center for Biochip at Shanghai, Shanghai 201203, PRC
[d]Graduate School, Shanghai University of Traditional Chinese Medicine, Shanghai 201203, PRC
[e]Department of Nutrition, University of North Carolina at Greensboro, North Carolina Research Campus, Kannapolis, NC 28081, USA

Received 7 January 2009; accepted 27 August 2009

Abstract

Excessive energy intake greatly contributes to the development of nonalcoholic fatty liver disease (NAFLD) in modern society. To better understand the comprehensive mechanisms of NAFLD development, we investigated the metabolic alterations of rats with NAFLD induced by high-fat diet (HFD). Male Wistar rats were fed a HFD or standard chow for control. After 16 weeks, rat serum was collected for biochemical measurement. The rats' livers were resected and subjected to histology inspection and gene expression analysis with complementary DNA microarray and metabolic analysis with gas chromatography–mass spectroscopy. In HFD rats, the serum cholesterol, triglycerides, glucose, and insulin contents were increased; and the total cholesterol and triglycerides in the livers were also significantly increased. Complementary DNA microarray analysis revealed that 130 genes were regulated by HFD. Together with real-time reverse transcriptase polymerase chain reaction, lipid metabolism regulatory members like sterol regulatory element binding factor 1 and stearoyl–coenzyme A desaturase 1 had up-regulation, whereas others like peroxisome proliferator–activated receptor, carnitine palmitoyltransferase 1, and 3-hydroxy-3-methylglutaryl–coenzyme A reductase had repressed expression, in HFD rat livers. Metabolomic analysis showed that tetradecanoic acid, hexadecanoic acid, and oleic acid had elevation and arachidonic acid and eicosapentaenoic acid had decreased content in HFD rat livers. Amino acids including glycine, alanine, aspartic acid, glutamic acid, and proline contents were decreased. The integrative results from transcriptomic and metabolomic studies revealed that, in HFD rat livers, fatty acid utilization through β-oxidation was inhibited and lipogenesis was enhanced. These observations facilitated our understanding of the pathways involved in the development of NAFLD induced by HFD.

1. Introduction

Excessive energy intake is an important contributor to the increase in nonalcoholic fatty liver disease (NAFLD) in modern society. Despite its prevalence, the underlying mechanisms of NAFLD are not fully understood. In addition to lipid accumulation in the liver caused by an excess intake of dietary fat, some lipid metabolism regulation genes associated with the development of NAFLD have been identified, such as genes encoding acyl–coenzyme A synthase, peroxisome proliferator–activated receptor γ, and SIRT1 protein [1-3]. These investigations have elucidated the path to the molecular mechanisms of NAFLD. However, this "gene-by-gene" strategy has constrained the research regarding the complex pathogenesis of NAFLD. Recent advances in high throughput "omic" technologies, including transcriptomics, proteomics, and metabolomics, have facilitated the assessment of multiple genes, proteins, and

* Corresponding authors. Tel.: +86 21 51320297; fax: +86 21 51320266.
E-mail addresses: w_jia@uncg.edu (W. Jia), qinghua_zhang@shbiochip.com (Q. Zhang).
[1] These authors contributed equally to the work.

0026-0495/$ – see front matter © 2010 Elsevier Inc. All rights reserved.
doi:10.1016/j.metabol.2009.08.022

metabolites simultaneously, which appears to be essential for understanding the biological mechanisms of complex diseases. Previous studies have shown the pleiotropic effects of a high-fat diet (HFD) producing global changes in gene expression profiles [4,5]. From a nutrigenomics perspective, nutrients are dietary signals that can be detected by the cellular sensor systems to influence gene and protein expression and, subsequently, metabolite production [6]. Thus, we propose that using the strategy of integrated omics technologies to document the global changes resulting from HFD feeding could provide comprehensive information to further the understanding of NAFLD pathogenesis.

Recently, we studied the different responses to long-term HFD feeding in a group of Wistar rats, that is, obesity-prone and obesity-resistant rats, with a transcriptomic and metabolomic approach. Our results indicated that various physiologic changes happened in obesity-prone rats, including increased activity of the sympathetic nervous system, Krebs cycle, and an increased production of ketone bodies as compared with the obesity-resistant rats, despite both groups of rats being fed an identical diet [7]. Accordingly, in the present study, we intend to investigate changes related to lipid metabolism in hepatic tissue induced by HFD feeding with combined transcriptomic and metabolomic approaches. The variations in gene expression and liver metabolites will provide information that may contribute to a better comprehension of the regulation pathways of molecular pathogenesis of NAFLD and become a basis for therapy and new drug development.

2. Materials and methods

2.1. Animal care and sample collection

The animal experiments were carried out under the Guidelines for Animal Experimentation of Shanghai University of Traditional Chinese Medicine (Shanghai, China), and the protocol was approved by the Animal Ethics Committee. Thirty 8-week-old male Wistar rats (210 ± 10 g) and animal food were commercially obtained from Shanghai Laboratory Animal. (SLAC, Shanghai, China). All animals were kept in a barrier system with regulated temperature (23°C-24°C) and humidity (60% ± 10%) and on a 12/12-hour light-dark cycle with lights on at 08:00 AM. The rats were fed with certified standard chow (SC) and tap water ad libitum for 1-week acclimation. Standard chow contains 22.10% crude protein, 50% carbohydrate, and 5.28% crude fat, whereas HFD was composed of 10% lard, 5% egg yolk powder, 2% cholesterol, and 83% SC (Supplementary material Table S1). Twenty rats were randomly selected and fed with HFD for 16 weeks, whereas the remaining 10 rats were fed SC over the experimental period. The body weight of each animal was measured weekly. At the end of the experiment, the animals were fasted overnight and then killed by anesthesia with sodium pentobarbital (100 mg/kg). Heparin anticoagulated plasma samples were collected, centrifuged (3000 rpm for 10 minute, 4 °C), and stored at −80°C. The livers were immediately weighed and frozen in liquid nitrogen and stored at −80°C for subsequent analysis. Formalin-fixed and paraffin-embedded livers were routinely processed for hematoxylin and eosin (H&E) staining.

2.2. Biochemical measurements

After overnight fasting, the lipid profile in rat serum, including triglycerides, total cholesterol, low-density lipoprotein cholesterol (LDL-c), and high-density lipoprotein cholesterol (HDL-c), was subjected to biochemical testing by routine procedures using a clinical biochemical analyzer (Roche Diagnostics, Mannheim, Germany) in Dongfang Hospital, Shanghai. At 15 weeks, rat serum glucose levels were measured with a handheld glucometer (Johnson & Johnson, Milpitas, CA) from whole blood drawn at the tail-tip capillary region; and insulin concentrations were measured at termination using a rat insulin radioimmunoassay kit (Dongya, Beijing, China). The analyzing process was conducted with strict adherence to the kits' instructions. The liver was homogenized in isopropanol at a concentration of 20 mg/mL and kept at 4°C for 2 hours. Afterward, the sample was centrifuged at 5000*g* for 15 minutes; and the suspension was collected for subsequent determination of cholesterol and triglycerides content in the liver by colorimetric method using cholesterol/triglycerides detection kit (Jiemen Biotech, Shanghai, China).

2.3. Microarray analysis

The rat complementary DNA microarray (Shanghai Biochip, Shanghai, China) covering 11 060 genes and expressed sequence tags was used [8]. Total RNA was prepared from each rat's liver using Trizol reagent (Invitrogen, Carlsbad, CA), further purified with RNeasy Kit (Qiagen, Hilden, Germany), and checked with 2100 Bioanalyzer (Agilent Technologies, Palo Alto, CA). Two micrograms of total RNA was applied to amplify using Low RNA Input Linear Amplification Kit (Agilent Technologies). Equal amounts of the RNA from SC rats were pooled to serve as a reference sample and labeled with cyanine 5 (Cy5; GE Healthcare, Piscataway, NJ), whereas the RNA from 8 HFD rats was labeled with cyanine 3 (Cy3, GE Healthcare) individually. The equivalent Cy5- and Cy3-labeled probes were mixed and hybridized at 42°C for 16 hours, and washed using standard protocol. The microarray slides were scanned with Agilent G2565BA Scanner, and the image data were extracted using ImaGene 4.2 (Biodiscovery, Santa Monica, CA).

2.4. Real-time reverse transcriptase polymerase chain reaction

Reverse transcription was performed with total RNA, oligo (dT) primers, and Superscript II reverse transcriptase (Invitrogen). Real-time reverse transcriptase polymerase chain reaction (RT-PCR) based on SYBR Green II

(Toyobo, Tokyo, Japan) was used to verify the results of microarray with the ABI Prism 7000 Sequence Detection System (Applied Biosystems, Foster City, CA). RNA samples from 3 rats in both the HFD and SC groups were tested. Gene expression was normalized to the expression of *Gapdh* as internal control; and subsequently, the data were analyzed using the comparative threshold cycle method. The PCR primer sequences are listed in Supplementary material Table S2.

2.5. Metabolic profiling of liver tissue extracts

Gas chromatography–mass spectroscopy (GC/MS)–based metabolic profiling was performed on the liver tissue extracts with established methods [9]. Liver tissue extracts were derivatized with ethylchloroformate (ECF) before instrumental analysis. Briefly, 600-μL aqueous extraction of liver tissue was added with 100 μL of L-2-chlorophenylalanine (0.10 mg/mL, internal standard for batch quality control), 400 μL of alcoholic extraction of liver tissue, and 100 μL of pyridine; derivatized with 50 μL of ECF at room temperature; and then ultrasonicated at 100 kHz for 60 seconds. The derivatives were extracted with 300 μL of chloroform, and the pH was adjusted with 100 μL of NaOH (7 mol/L). The derivatization process was repeated by adding an additional 50 μL of ECF. The resultant mixtures were centrifuged at 3000 rpm for 3 minutes. Afterward, the aqueous layer was aspirated, whereas the chloroform layer containing derivatives was dehydrated with anhydrous sodium sulfate for subsequent instrumental analysis.

2.6. Data analysis

The microarray data were processed as before [10]. After normalization of the Cy3 and Cy5 signals between and within chips with LOWESS progression, the Cy3/Cy5 signal ratios were log [2] transformed. Afterward, we applied the Significance Analysis of Microarray version 2.2.1 protocol [11] to pick out the statistically significant gene expression regulations and took the 1-class analysis at false discovery rate = 0.01, plus an average cutoff of 1.5-fold changes. All gene expression information in the experiment had been submitted to the Gene Expression Omnibus database with the registration no. GSE11492. The spectral processing and multivariate statistics for GC/MS-based metabolic profiling were performed with Matlab (The MathWorks, Inc, Natick, MA) and SIMCA-P Software package (Umetrics, Umeå, Sweden) as previously reported [12].

3. Results

3.1. Phenotypic and biochemical parameters

After 16 weeks, the HFD rats developed significantly higher body and liver weight in comparison with SC rats, although they consumed the same amount of food. The total cholesterol and triglyceride liver contents were increased by 25.7-fold (2.1 vs 54.1 mg/g liver, $P < .01$) and 8.5-fold (12.4 vs 105.5 mg/g liver, $P < .01$), respectively. Accordingly, histologic staining of liver tissue with H&E staining showed obvious fat droplet accumulation in livers of HFD-feeding rat (Fig. 1). The total cholesterol, LDL-c, triglycerides, glucose, and insulin were increased in the HFD-fed group, whereas the HDL-c was decreased (Table 1).

3.2. Transcriptomic profiles of rat liver

Using SAM software analysis, 130 genes were selected to have more than 1.5-fold regulation. Among the regulated genes, the highest proportions were those related to lipid metabolism (Table 2 and Supplementary material Table S3). As a consequence of HFD feeding, liver lipid metabolism involving genes were mainly regulated. Cholesterol biosynthesis participating members, for example, 3-hydroxy-3-methylglutaryl–coenzyme A synthase 1, sterol-c4-methyl oxidase-like, isopentenyl-diphosphate δ isomerase, and emopamil binding protein, had decreased expression. The down-regulation also happened in steroid metabolism genes, including cytochrome P450, family 17, subfamily A, polypeptide 1; cytochrome P450, family 8, subfamily B, polypeptide 1; and hydroxysteroid (17-β) dehydrogenase 2, and the genes encoding fatty acid metabolism enzymes, such as fatty acid desaturase 1 (*Fads1*), enoyl coenzyme A hydratase 1 (*Ech1*), and dodecenoyl–coenzyme A δ isomerase (*Dci*). Significantly, sterol regulatory element

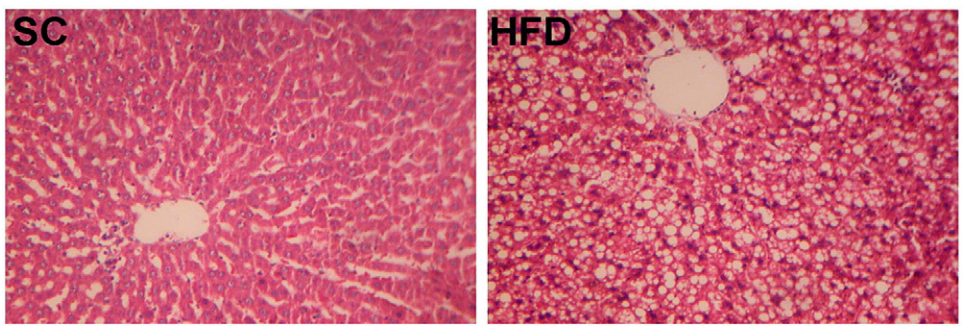

Fig. 1. Histologic detection of the rat livers. Rat livers were stained with H&E. Lipid droplets were obviously accumulated in HFD rats, but not SC rats (original magnification ×100).

Table 1
Phenotypic and biochemical parameters

Items	SC rats (n = 10)	HFD rats (n = 20)
Daily food intake (g)	22 ± 2	23 ± 3
Body weight (g)		
Initial	246 ± 7.8	253.1 ± 11
Final	440.8 ± 15.6	481.7 ± 39.0*
Liver		
Liver weight (g/100g body weight)	2.34 ± 0.15	3.38 ± 0.17†
Triglycerides (mg/g liver)	12.4 ± 3.1	105.5 ± 22.0†
Total cholesterol (mg/g liver)	2.1 ± 0.33	54.1 ± 8.7†
Serum		
Total cholesterol (mmol/L)	1.61 ± 0.41	1.95 ± 0.19†
HDL-c (mmol/L)	1.39 ± 0.30	1.11 ± 0.27*
LDL-c (mmol/L)	0.18 ± 0.10	0.64 ± 0.16†
Triglycerides (mmol/L)	0.84 ± 0.30	1.26 ± 0.36†
Glucose (mmol/L)	5.14 ± 0.34	5.5 ± 0.26†
Insulin (μU/mL)	48.45 ± 6.80	57.60 ± 7.25*

Data are presented as means ± SD. Comparison was made between HFD rats and SC rats by 2-tailed Student *t* test.

* $P < .05$.

† $P < .01$.

binding factor 1 (*Srebf1*) had increased expression, whereas expression of insulin-induced gene 1 (*Insig1*) was repressed.

Although no significant alterations of liver function parameters were detected in HFD rat (data not shown), inflammatory and stress response member genes were also detected. The acute inflammation cytokine chemokine (c-x-c motif) ligand 1 (*Cxcl1*) and complement regulator complement component factor h (*Cfh*) had up-regulation; the macrophage homeostasis cytokine chemokine (c-x-c motif) ligand 14 was repressed. In addition, stress response–associated encoding genes like RB2-associated binding protein 1, growth arrest and DNA-damage–inducible 45 γ, and cold inducible RNA binding protein showed increased expression, whereas heat shock protein 1 was decreased.

In addition to the results obtained with complementary DNA microarray, we conducted real-time RT-PCR for 12 lipid metabolism–associated genes and 6 antioxidant enzyme genes. The results showed a high consistency with the microarray data. Peroxisome proliferator–activated receptor (*Ppara*), carnitine palmitoyltransferase 1 (*Cpt1*), and 3-hydroxy-3-methylglutaryl–coenzyme A reductase had repression; and the lipogenesis transcription factor *Srebf1* and stearoyl–coenzyme A desaturase 1 (*Scd1*) had significant up-regulation (Fig. 2). No significant regulations at gene expression level were found for the detected antioxidant enzymes (Supplementary material Figure S1).

3.3. Metabolomic profile of liver tissue extracts

With GC/MS strategy, we identified that 5 long-chain fatty acids and 5 amino acids have significant differential contents in rat liver extracts (Table 3). In HFD rats, the liver had much higher contents of tetradecanoic acid (14:0), hexadecanoic acid (16:0), and oleic acid (18:1), but lower contents of polyunsaturated fatty acids, arachidonic acid (AA) (20:4), and eicosapentaenoic acid (EPA) (20:5). The liver contents of glucogenic amino acids including glycine, alanine, proline, glutamine acid, and aspartate acid were much lower in HFD rats compared with the SC rats.

4. Discussion

Nonalcoholic fatty liver disease is a common disease characterized by excessive triglyceride accumulation in the liver. Given the complexity of the pathogenesis of NAFLD, our study adopted a strategy of combined analysis of transcriptomic and metabolomic profiling for investigating NAFLD. After 16 weeks of HFD feeding, the plasma levels of lipids, glucose, and insulin were significantly increased. Furthermore, comprehensive variations were observed in the liver of rats subjected to long-term HFD feeding, including genes involved in cellular lipid metabolism, inflammation, and stress response. These observations increased our

Table 2
Differentially expressed genes between HFD and SC rats

Gene	Description	Fold change (HFD/SC)
Lipid metabolism		
Insig1	Insulin-induced gene 1	0.406
Sc4mol	Sterol-c4-methyl oxidase-like	0.490
Idi1	Isopentenyl-diphosphate δ isomerase	0.640
Cyp17a1	Cytochrome p450, family 17, subfamily a, polypeptide 1	0.600
Fads1	Fatty acid desaturase 1	0.631
Ech1	Enoyl coenzyme a hydratase 1, peroxisomal	0.597
Mtmr4	Myotubularin-related protein 4	1.523
LOC246266	Lysophospholipase	0.395
Cyp8b1	Cytochrome p450, family 8, subfamily b, polypeptide 1	0.580
Srebf1	Sterol regulatory element binding factor 1	2.140
Ebp	Phenylalkylamine Ca2+ antagonist (emopamil) binding protein	0.625
Nr1i2	Nuclear receptor subfamily 1, group i, member 2	0.662
Dci	Dodecenoyl–coenzyme A δ isomerase	0.409
Hmgcs1	3-Hydroxy-3-methylglutaryl–coenzyme A synthase 1	0.576
Hsd17b2	Hydroxysteroid (17-β) dehydrogenase 2	0.656
Ephx2	Epoxide hydrolase 2, cytoplasmic	0.664
Inflammation and stress response		
Cxcl14	Chemokine (c-x-c motif) ligand 14	0.610
Cfh	Complement component factor h	1.680
Cxcl1	Chemokine (c-x-c motif) ligand 1	2.886
Ptger3	Prostaglandin e receptor 3 (subtype ep3)	0.578
Tollip	Toll interacting protein	0.631
Gab1	GRB2-associated binding protein 1	1.605
Gadd45g	Growth arrest and DNA-damage-inducible 45 γ	2.963
Nfe2l2	Nuclear factor, erythroid derived 2, like 2	1.693
Cirbp	Cold inducible RNA binding protein	1.562
Hsph1	Heat shock 105 kd/110 kd protein 1	0.649

Differentially expressed genes with a regulation of at least 1.5 between HFD and SC rats are represented. The fold change represents the relative gene expression in HFD rats compared with SC rats.

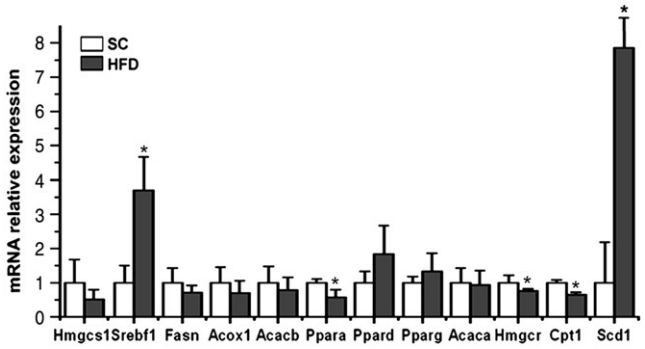

Fig. 2. Real-time RT-PCR detection of lipid metabolism–related genes. The gene expression is the relative average ΔCT as normalized to the corresponding *Gapdh*; each gene in the SC group was set as 1. *$P < .05$.

understanding of the pathways involved in the development of NAFLD induced by HFD.

We found that genes involved in fatty acid β-oxidation were coordinately down-expressed, that is, *Ppara*, *Cpt1*, *Ech1*, and *Dci*. *Ppara* encodes a transcription factor that regulates genes involved in fatty acid uptake and β-oxidation [13,14]; *Ppara*-null mice chronically fed an HFD showed a massive accumulation of lipid in their livers[15]. Unsaturated long-chain fatty acids are endogenous ligands of *Ppara* with a high affinity for promoting *Ppara*-mediated fatty acid β-oxidation in the liver [16]. As a result, the decrease of polyunsaturated long-chain fatty acids such as AA and EPA, as well as the down-expression of *Ppara* and its target genes such as *Cpt1* (the rate-limiting enzyme in fatty acid β-oxidation [17]), suggested the decreased β-oxidation of fatty acids in HFD rats. The higher concentrations of long-chain fatty acids such as tetradecanoic acid (14:0), hexadecanoic acid (16:0), and oleic acid (18:1) in the liver could result from excess fat intake and/or decreased fatty acid β-oxidation in HFD rats. Collectively, the gene expression and metabolite profiles consistently suggested the decreased β-oxidation of fatty acid after long-term HFD feeding.

Arachidonic acid and EPA are downstream products of essential fatty acids including linoleic acid and α-linolenic acid [18]. As HFD rats took in the same amount of food as SC rats, the lesser proportion of polyunsaturated fatty acid in HFD might result in the decrease of AA and EPA in HFD rat livers. Furthermore, the repressed expression of *Fads1*, which participates in the synthesis of polyunsaturated fatty acids, could contribute to the decrease of AA and EPA. Stearoyl–coenzyme A desaturase 1, a δ-9 fatty acid desaturase, converts saturated fatty acids into monounsaturated fatty acids. It has been suggested that its activity influences fatty acid partitioning by promoting fatty acid synthesis but decreasing β-oxidation. The expression *Scd1* was shown to be induced by saturated fatty acids [19-21]. Thus, increased saturated fatty acids like tetradecanoic acid (14:0) and hexadecanoic acid (16:0) may have contributed to the overexpression of *Scd1*, which subsequently induced the increase of oleic acid (18:1) in rat livers. In addition, the increased expression of *Scd1* could have contributed to the elevated plasma insulin and glucose levels in HFD rats, which have been shown to be related to the onset of diet-induced hepatic insulin resistance [22,23]. Srebp1 controls cholesterol homeostasis by stimulating the transcription of sterol-regulated genes [24], thus regulating lipid biosynthesis [25]. *Insig1* binds to the sterol-sensing domains of SREBP cleavage-activating protein and is essential for the retention of the protein in endoplasmic reticulum [26]. Taken together, the overexpression of *Srebf1* and down-expression of *Insig1* may promote the lipogenesis in rat liver.

In our experiment, we found that glucogenic amino acids decreased whereas lipids accumulated in HFD rat liver tissues, which symphonized with the elevation of serum lipids, glucose, and insulin, although no significant expression regulations of the glyconeogenesis-participating enzymes were found (data not shown). This was consistent with the hypoaminoacidemic effect involved in glucogenic amino acids by lipid over administration [27] and the elevation of plasma glucogenic amino acids caused by acute caloric restriction [28]. As PPARα deficiency could develop mice obesity but protect mice from insulin resistance caused by being fed an HFD [29], and PPARα agonist could increase plasma levels of amino acids [30], the repressed expression of PPARα placed a protective role for the lipid and glucose metabolism regulation network.

Although no significantly elevated levels of liver damage marker enzymes alkaline phosphatase, aspartate transaminase, and alanine transaminase were detected (data not shown), inflammation is still thought to play an important role in the progression from hepatic steatosis to nonalcoholic steatohepatitis [31]. In this study, we observed a number of differentially expressed genes involved in inflammation and stress response in HFD rat livers, such as the up-regulated expression of *Cxcl1*, which is a neutrophil chemoattractant that plays a role in acute phase

Table 3
Differential metabolites in liver between HFD and SC rats

Metabolites	RT/min	Fold change (HFD/SC)
Fatty acids		
Tetradecanoic acid	17.34	3.6
Hexadecanoic acid	22.11	4.5
Oleic acid	25.88	2.8
AA	28.99	0.4
EPA	32.71	0.3
Amino acids		
Glycine	7.6	0.6
Alanine	7.49	0.7
Aspartic acid	14.08	0.4
Glutamic acid	16.78	0.5
Proline	24.06	0.6

Differential metabolites between HFD (n = 20) rats and SC (n = 10) rats were identified with O-PLS-DA on SIMCA-P software. RT/min indicates retention time (minutes) on gas chromatograph. Fold change HFD/SC represents the HFD/SC ratio of the relative concentrations of differential metabolites between HFD and SC groups.

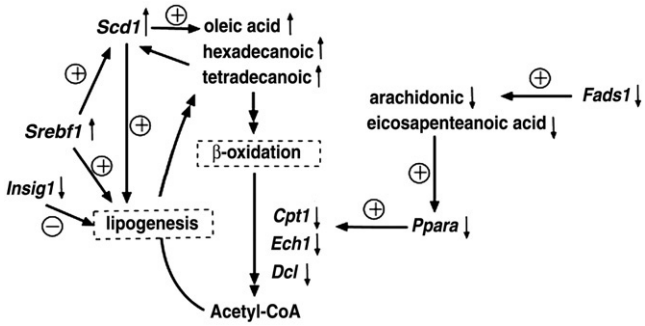

Fig. 3. Ideogram illustration of integrated gene expressions and metabolites in HFD rat liver. The bioprocess is represented as dashed rectangles; the metabolites, as names; and the genes, as symbols. The arrows indicate the content or expression regulations, and the "+" and "−" indicate the positive or negative regulatory functions.

inflammatory response [32,33], and *Cfh*, which encodes complement component factor h to facilitate complement-mediated cascade activation. Oxidative stress was one of the important factors in NAFLD development; and decreased activities of superoxide dismutase, glutathione peroxidase, and glutathione-*S*-transferase were often reported. In our study, at the gene expression level, no significant expression regulations were detected in the HFD rat livers (Supplementary material Figure S1).

This study measured the variations in the metabolomic and transcriptomic profiles of HFD-fed rats relative to the control group fed with standard rat chow. Such variations in liver metabolome and transcriptome were caused by the dietary content of 10% lard, 5% egg yolk powder, and 2% cholesterol (whereas the other 83% remained the same as standard rat chow) and therefore may not readily mimic the biochemical variations of NAFLD phenotype. However, these variations assessed by the 2 profiling approaches are correlated with each other and consistent with the relevant studies of HFD-induced fatty liver [34,35]. The contribution of "exogenous" metabolites from dietary amino and fatty acids in our metabolic data was eliminated, as our analyses only focused on the liver tissues instead of biofluids such as blood and urine.

In conclusion, we demonstrated through the integrated study of transcriptome and metabolome profiles that long-term HFD feeding results in multidimensional alterations in rat livers. Especially fatty acid metabolism, such as inhibited β-oxidation and enhanced lipogenesis (Fig. 3), and inflammatory and stress responses–related genes are regulated. Further investigations of these differentially expressed genes and metabolic pathways are of particular significance in the mechanistic study of HFD-induced NAFLD.

Acknowledgment

This work was financially supported by the Development Projects of Shanghai Commission of Science and Technology (06DZ19727), the National Basic Research Program of China (973-2007CB914700), and the International Collaborative Project of Chinese Ministry of Science and Technology (2006DFA02700). Here, on behalf of all authors, I declare that no competing interest exists.

Appendix A. Supplementary data

Supplementary data associated with this article can be found, in the online version, at doi:10.1016/j.metabol.2009.08.022.

References

[1] Ikemoto S, Takahashi M, Tsunoda N, et al. Cholate inhibits high-fat diet–induced hyperglycemia and obesity with acyl-CoA synthetase mRNA decrease. Am J Physiol 1997;273:E37-45.
[2] Matsui J, Terauchi Y, Kubota N, et al. Pioglitazone reduces islet triglyceride content and restores impaired glucose-stimulated insulin secretion in heterozygous peroxisome proliferator-activated receptor-gamma–deficient mice on a high-fat diet. Diabetes 2004;53:2844-54.
[3] Deng XQ, Chen LL, Li NX. The expression of SIRT1 in nonalcoholic fatty liver disease induced by high-fat diet in rats. Liver Int 2007;27:708-15.
[4] Koza RA, Nikonova L, Hogan J, et al. Changes in gene expression foreshadow diet-induced obesity in genetically identical mice. PLoS Genet 2006;e81:2.
[5] Sparks LM, Xie H, Koza RA, Mynatt R, Bray GA, Smith SR. High-fat/low-carbohydrate diets regulate glucose metabolism via a long-term transcriptional loop. Metabolism 2006;55:1457-63.
[6] Muller M, Kersten S. Nutrigenomics: goals and strategies. Nat Rev Genet 2003;4:315-22.
[7] Li H, Xie Z, Lin J, et al. Transcriptomic and metabonomic profiling of obesity-prone and obesity-resistant rats under high fat diet. J Proteome Res 2008;7:4775-83.
[8] Li RY, Zhang QH, Liu Z, et al. Effect of short-term and long-term fasting on transcriptional regulation of metabolic genes in rat tissues. Biochem Biophys Res Commun 2006;344:562-70.
[9] Qiu Y, Su M, Liu Y, et al. Application of ethyl chloroformate derivatization for gas chromatography–mass spectrometry based metabonomic profiling. Anal Chim Acta 2007;583:277-83.
[10] Gu X, Xie Z, Wang Q, et al. Transcriptome profiling analysis reveals multiple modulatory effects of *Ginkgo biloba* extract in the liver of rats on a high-fat diet. Febs J 2009;276:1450-8.
[11] Tusher VG, Tibshirani R, Chu G. Significance analysis of microarrays applied to the ionizing radiation response. Proc Natl Acad Sci U S A 2001;98:5116-21.
[12] Lickteig AJ, Fisher CD, Augustine LM, Cherrington NJ. Genes of the antioxidant response undergo upregulation in a rodent model of nonalcoholic steatohepatitis. J Biochem Mol Toxicol 2007;21:216-20.
[13] Lee CH, Olson P, Evans RM. Minireview: lipid metabolism, metabolic diseases, and peroxisome proliferator–activated receptors. Endocrinology 2003;144:2201-7.
[14] Yu S, Rao S, Reddy JK. Peroxisome proliferator–activated receptors, fatty acid oxidation, steatohepatitis and hepatocarcinogenesis. Curr Mol Med 2003;3:561-72.
[15] Kersten S, Seydoux J, Peters JM, Gonzalez FJ, Desvergne B, Wahli W. Peroxisome proliferator–activated receptor alpha mediates the adaptive response to fasting. J Clin Invest 1999;103:1489-98.
[16] Hostetler HA, Petrescu AD, Kier AB, Schroeder F. Peroxisome proliferator–activated receptor alpha interacts with high affinity and is conformationally responsive to endogenous ligands. J Biol Chem 2005;280:18667-82.

[17] Jambor de Sousa UL, Koss MD, Fillies M, et al. CPT1alpha over-expression increases long-chain fatty acid oxidation and reduces cell viability with incremental palmitic acid concentration in 293T cells. Biochem Biophys Res Commun 2005;338:757-61.
[18] Das UN. Essential fatty acids—a review. Curr Pharm Biotechnol 2006;7:467-82.
[19] Flowers MT, Ntambi JM. Stearoyl-CoA desaturase and its relation to high-carbohydrate diets and obesity. Biochim Biophys Acta 1791;2009:85-91.
[20] Sampath H, Miyazaki M, Dobrzyn A, Ntambi JM. Stearoyl-CoA desaturase-1 mediates the pro-lipogenic effects of dietary saturated fat. J Biol Chem 2007;282:2483-93.
[21] Li ZZ, Berk M, McIntyre TM, Feldstein AE. Hepatic lipid partitioning and liver damage in nonalcoholic fatty liver disease: role of stearoyl-CoA desaturase. J Biol Chem 2009;284:5637-44.
[22] Gutierrez-Juarez R, Pocai A, Mulas C, et al. Critical role of stearoyl-CoA desaturase-1 (SCD1) in the onset of diet-induced hepatic insulin resistance. J Clin Invest 2006;116:1686-95.
[23] Warensjo E, Ingelsson E, Lundmark P, et al. Polymorphisms in the SCD1 gene: associations with body fat distribution and insulin sensitivity. Obesity (Silver Spring) 2007;15:1732-40.
[24] Eberle D, Hegarty B, Bossard P, Ferre P, Foufelle F. SREBP transcription factors: master regulators of lipid homeostasis. Biochimie 2004;86:839-48.
[25] Magana MM, Koo SH, Towle HC, Osborne TF. Different sterol regulatory element-binding protein-1 isoforms utilize distinct co-regulatory factors to activate the promoter for fatty acid synthase. J Biol Chem 2000;275:4726-33.
[26] Yang T, Espenshade PJ, Wright ME, et al. Crucial step in cholesterol homeostasis: sterols promote binding of SCAP to INSIG-1, a membrane protein that facilitates retention of SREBPs in ER. Cell 2002;110:489-500.
[27] Ferrannini E, Barrett EJ, Bevilacqua S, et al. Effect of free fatty acids on blood amino acid levels in human. Am J Physiol 1986;250:E686-94.
[28] Selman C, Kerrison ND, Cooray A, et al. Coordinated multitissue transcriptional and plasma metabonomic profiles following acute caloric restriction in mice. Physiol Genomics 2006;27:187-200.
[29] Finck BN, Bernal-Mizrachi C, Han DH, et al. A potential link between muscle peroxisome proliferator–activated receptor–alpha signaling and obesity-related diabetes. Cell Metab 2005;1:133-44.
[30] Sheikh K, Camejo G, Lanne B, Halvarsson T, Landergren MR, Oakes ND. Beyond lipids, pharmacological PPARalpha activation has important effects on amino acid metabolism as studied in the rat. Am J Physiol Endocrinol Metab 2007;292:E1157-65.
[31] Rector RS, Thyfault JP, Wei Y, Ibdah JA. Non-alcoholic fatty liver disease and the metabolic syndrome: an update. World J Gastroenterol 2008;14:185-92.
[32] Campbell SJ, Hughes PM, Iredale JP, et al. CINC-1 is an acute-phase protein induced by focal brain injury causing leukocyte mobilization and liver injury. Faseb J 2003;17:1168-70.
[33] Kaibori M, Yanagida H, Nakanishi H, et al. Hepatocyte growth factor stimulates the induction of cytokine-induced neutrophil chemoattractant through the activation of NF-kappaB in rat hepatocytes. J Surg Res 2006;130:88-93.
[34] Gauthier MS, Favier R, Lavoie JM. Time course of the development of non-alcoholic hepatic steatosis in response to high-fat diet-induced obesity in rats. Br J Nutr 2006;95:273-81.
[35] Buettner R, Parhofer KG, Woenckhaus M, et al. Defining high-fat-diet rat models: metabolic and molecular effects of different fat types. J Mol Endocrinol 2006;36:485-501.